

# A Ripple Free Soft-Switched Integrated Series Resonant Converter for Main and Local LED Lighting Application

Narender Jatoth<sup>1</sup>, K Ravikumar<sup>2</sup>, M Manjula<sup>1</sup>

<sup>1</sup>*Department of Electrical Engineering, Osmania University, India*

<sup>2</sup>*Department of Electrical & Electronics Engineering, Vasavi College of Engineering, India*

*Email: narenderjatoth@gmail.com*

Light emitting diode (LED) lighting industry demands efficient driver circuits to suit various lighting applications. The requirements of applications like factory lighting, loco sheds, main office buildings etc are different. In such applications, main lighting system must be operated at full illumination and local lighting must be controllable. In this research work, an integrated full-bridge series resonant converter with zero-voltage switching (ZVS) is proposed to power both local and main lighting systems. Two main lamps are powered using inter-leaving concept. Local lighting is supplied through series LC resonant circuit. Lamps or strings in local lighting are dimmed independently. Both main and local lighting can be regulated using a modified buck-boost converter which is connected in series with input voltage. The ZVS feature of devices in full-bridge converter is independent of local LED string currents. In addition conduction losses mainly depend on the magnitude of local LED string current. Therefore high conversion efficiency is possible due to low conduction and switching transition power losses. Numerical simulations are conducted using ORCAD simulation environment and results are used for the validation of proposed resonant converter topology for LED applications.

**Keywords:** Zero Voltage Switching, Resonant converters, Light emitting diodes and Dimming Control.

## 1. Introduction

Lighting loads consume approximately 20% of total electrical energy generated across the world [1-2]. Thus there is enough scope to enhance the energy conservation through lighting appliances. Most of the lighting applications are occupied by LEDs due to their features such as long life, faster dynamic response, low carbon emission, energy efficient light source, and environment friendly etc. [3]–[6]. Owing to their benefits, LEDs are certainly substituting traditional lighting systems in automotive, streetlight, residential, factory and decorative applications, etc. [7]–[9].

LEDs forward voltage and current characteristics are similar to p-n junction diode [10].

Moreover illumination output from LEDs depends on forward current. In many applications, the operating current of LEDs must be constant and regulated. Hence LED lighting systems are powered from constant current regulators. They are also called LED driver circuits. Mostly switched mode power electronic converters are used to drive LED lighting systems.

Different driver circuits have been proposed for different LED lighting applications [11-19]. Input modulated full bridge driver circuits with soft-switching feature are presented to power multiple identical LED lamps [11-12]. A ripple free LED driver with ZVS feature and reduced current stress for street lighting application is proposed [13]. However LED lamps are identical and independent dimming and regulation are not addressed. A variable frequency controlled high gain integrated buck-boost series resonant converter is used for powering multiple LED loads [14]. Two LED lamps with different wattage are supplied from coupled inductor based driver circuit with soft-switching [15]. In this paper, leakage energy is used to power one LED lamp which limits its rating. The author in [16] address to drive two identical lamps with independent dimming with half bridge LC resonant circuit. A multi-output zero voltage switched dc-dc converter for LED lighting application using variable inductor is implemented [17]. Independent dimming, regulation, ZVS feature, etc. are achieved. However variable inductor design and implementation require additional control circuit. Two different wattage lamps are supplied using three leg resonant LED converter [18]. It features independent operation, dimming and regulation. But the current stress of devices in common leg is high and also their ZVS feature is not complete. A half bridge resonant converter for two loads is presented in [19]. The major benefits are drives two loads with independent control, however the switching logic for independent control makes complex.

Despite the availability of different LED driver circuits, some applications like factory lighting, loco sheds, main office buildings, etc. need converter circuits to fulfil their objectives. In this paper, an integrated full-bridge series resonant LED driver circuit is presented to power both local and main lighting systems. In this configuration, input voltage is modulated to control the currents in both main and local lighting systems. Independent PWM dimming is implemented for only local lighting and main lighting is operated at full illumination. The organization of the paper is as follows, working principle of proposed converter is presented in section 2, followed by mathematical analysis and design parameters of proposed converter is presented in section 3 and section 4 respectively. Section 5 describes the dimming control and current regulation. The results and discussions are presented in section 6. Finally, the conclusions are presented in section 7.

## **2. Proposed Integrated Series Resonant Converter**

### **A. Description**

Figure 1 shows the proposed converter configuration for driving main and local lighting. It is developed with full bridge inverter (FBI) with four MOSFETs ( $Q_1$ - $Q_4$ ) and series resonant circuit (SRC). Each MOSFET in FBI is represented with an intrinsic body diode and output capacitance. SRC is formed by resonant inductor ( $L_r$ ), resonant capacitor ( $C_r$ ) and current driven full bridge rectifier ( $D_{B1}$ - $D_{B4}$ ). The  $V_{AC}$  is output voltage of FBI. Two local LED strings (LLS) are supplied through SRC. Switches  $S_{dim1}$  and  $S_{dim2}$  are used to dim LLS independently.

The voltage of LLS is represented by  $V_{LLS}$  and current in LLS-1 and LLS-2 are represented by  $i_{LLS1}$  and  $i_{LLS2}$  respectively. The ripple in  $i_{LLS1}$  and  $i_{LLS2}$  is minimized by filter capacitor  $C_0$ . Two identical main lamps are used and powered by using multi-phasing or interleaving concept. Ripple free current flows in main lamp-1 due to  $180^\circ$  out of phase current in inductor  $L_1$  and  $L_1'$ . Similarly, the  $180^\circ$  out of phase current in inductor  $L_2$  and  $L_2'$  makes current in main lamp-2 ripple free. The output voltage/current of main lamp-1 and lamp-2 are represented by  $V_{m1}/i_{m1}$ , and  $V_{m2}/i_{m2}$ , respectively. In proposed configuration, input voltage is modulated for regulating both main and local lighting systems. The input voltage ( $V_{DC}$ ) to the FBI is made into the sum of three voltages  $V_{in1}$ ,  $V_{in2}$  and  $V_C$ . A modified conventional buck-boost with input voltage  $V_{in2}$  generates a controllable voltage  $V_C$ , which can compensate the variations in  $V_{in1}$  &  $V_{in2}$ .

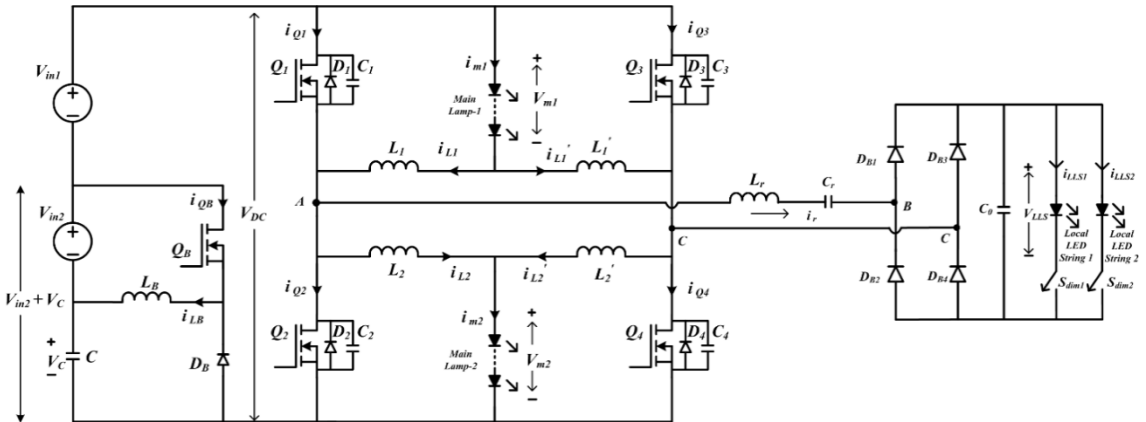


Figure 1. Proposed resonant LED driver

## B. Operation of Proposed Configuration

The gate voltage ( $v_{g1}$  &  $v_{g2}$ ) of equal width with small dead time are applied complementarily for devices  $Q_1$  and  $Q_2$  respectively. Similarly,  $v_{g3}$  and  $v_{g4}$  are given complementarily for  $Q_3$  and  $Q_4$ . The resonant frequency ( $f_0$ ) of SRC is selected same as switching frequency ( $f_s$ ). The operation of proposed configuration in a switching period ( $T_s$ ) is divided into four modes. Operating waveforms and equivalent circuit in each mode are shown in Figure 2 and Figure 3 & 4 respectively. The operating mode are explained in this section.

### Mode I

At time  $t=t_0$ , gate voltages to switches  $Q_1$  &  $Q_4$  are given and start conduction at zero voltage. From the operative circuit shown in Figure 3(a), the FBI output voltage ( $V_{AC}$ ) is  $+V_{DC}$  and is given to SRC. Thus a positive sinusoidal resonant current  $i_r$  is produced and drives local LED strings through  $D_{B1}$  &  $D_{B4}$ . At the same time, interleaving inductors ( $L_1$  &  $L_1'$ ) of main lamp-1 discharge and charge linearly. Similarly, ( $L_2$  &  $L_2'$ ) of main lamp-2 charge and discharge respectively. Switch  $Q_1$  conducts the sum of resonant current  $i_r$  and the difference ( $i_{L1} - i_{L2}$ ) between inductor  $L_1$  and  $L_2$  current. And switch  $Q_4$  conducts the sum of resonant current  $i_r$  and the difference ( $i_{L2}' - i_{L1}'$ ) between inductor  $L_2'$  and  $L_1'$ . At  $t = t_1$ , gate voltages  $v_{g1}$  and  $v_{g4}$  are removed.

### Mode II

At  $t = t_1$ ,  $Q_1$  and  $Q_4$  are stopped conduction at zero voltage. From the operative circuit shown in Figure 3(b), the output capacitance of  $Q_1$  and  $Q_4$  are charged by currents  $(i_{L2} - i_{L1})/2$  and  $(i_{L1} - i_{L2})/2$  from zero to  $V_{DC}$ . At the same instant, output capacitance of  $Q_2$  and  $Q_3$  discharged by  $(i_{L2} - i_{L1})/2$  and  $(i_{L1} - i_{L2})/2$  from  $V_{DC}$  to zero. When the voltage across body diode of  $Q_2$  and  $Q_3$  greater than  $-0.7$  V,  $D_2$  and  $D_3$  are forward biased. Now gate voltages for switches  $Q_2$  and  $Q_3$  may be given for zero voltage turn on. This mode ends at  $t = t_2$ .

### Mode III

During  $t_2 - t_3$ , switches  $Q_2$  &  $Q_3$  are conducting. The operative circuit is shown in Figure 4(a). The FBI output voltage ( $v_{AC}$ ) is  $-V_{DC}$  and is applied to SRC. Thus negative sinusoidal resonant current  $i_r$  is generated and it forward biases diodes  $D_{B2}$  &  $D_{B3}$  and supplies local LED strings. In this mode, interleaving inductor  $L_1$  of main lamp-1 charges through  $Q_2$  and  $L_1'$  of main lamp-1 discharges through  $Q_3$ . Similarly,  $L_2$  of main lamp-2 discharges through  $Q_2$  and  $L_2'$  of main lamp-2 charges through  $Q_3$ . Switch  $Q_2$  carries sum of  $i_r$  and the difference between current  $i_{L2}$  and  $i_{L1}$ . And switch  $Q_3$  carries sum of  $i_r$  and the difference between  $i_{L1}'$  and  $i_{L2}'$ . At  $t = t_3$ , gate voltages  $v_{g2}$  and  $v_{g3}$  are removed at zero voltage.

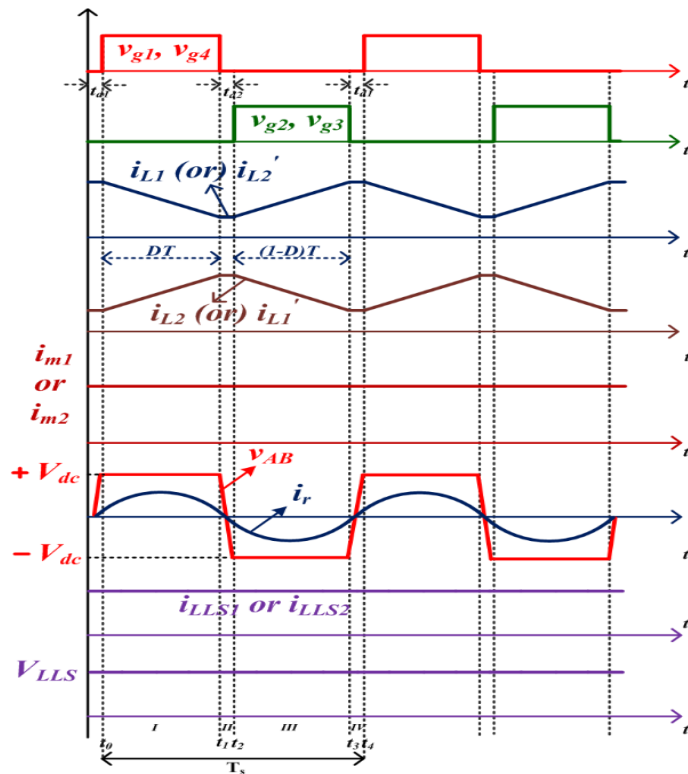


Figure 2. Operating waveforms

### Mode IV

From  $t_3 - t_4$ , no switch is conducting. The operative circuit is shown in Figure 4(b). In this

mode, output capacitance of  $Q_2$  and  $Q_3$  are charged from zero to  $V_{DC}$  by currents  $(i_{L1}-i_{L2})/2$  and  $(i_{L2}'-i_{L1}')/2$  respectively. Similarly, output capacitance of  $Q_1$  and  $Q_4$  are discharged from  $V_{DC}$  to zero by  $(i_{L1}-i_{L2})/2$  and  $(i_{L2}'-i_{L1}')/2$  respectively. When voltage across  $C_1$  and  $C_4$  are less than  $-0.7$  V, body diodes  $D_1$  and  $D_4$  are forward biased. Now gate voltages for switches  $Q_1$  and  $Q_4$  may be given for zero voltage turn on. This mode ends at  $t = t_4$ .

### 3. Analysis of Proposed LED Driver

In order to make the analysis of proposed converter is simple, the following assumptions are made.

- (i) The converter is operating in steady state.
- (ii) All the switching components used are assumed to be ideal.
- (iii) The main lamps of the proposed converter are assumed to be identical.
- (iv) The local LED strings are assumed to be identical.
- (v) The voltage across local and main lighting systems are constant.

The switches in FBI are conducted with equal ON and OFF time duration at fixed frequency. Main and local lighting systems are used in the proposed converter. Thus, analysis is provided with respect to main and local lighting systems separately.

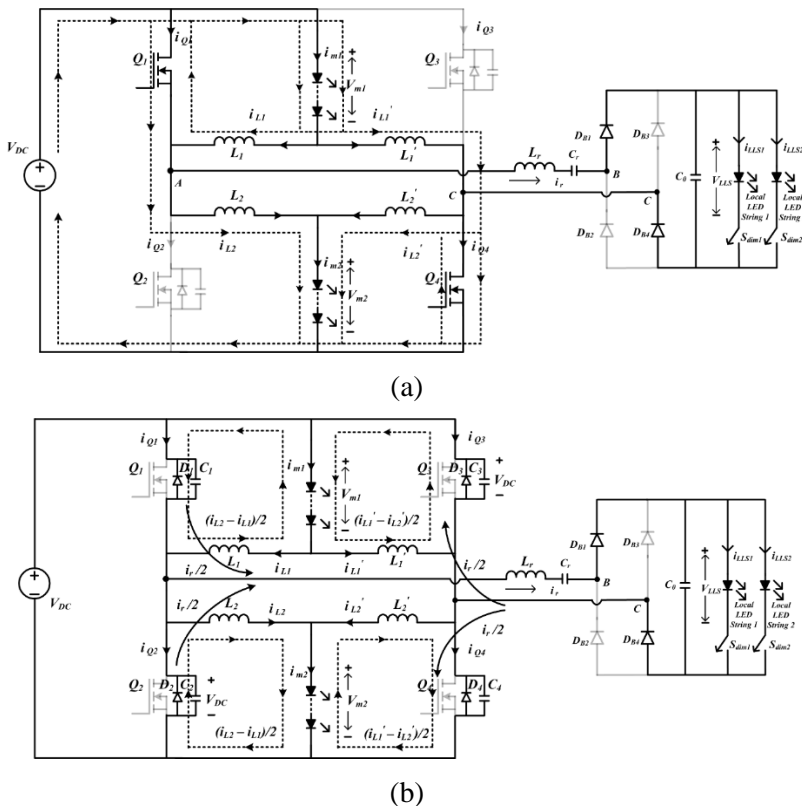


Figure 3. Operative circuits in(a) Mode I, (b) Mode II



$$v_{L1} = -V_{m1} = L_1 \frac{di_{L1}}{dt} \quad t_0 \leq t < t_1 \quad (1)$$

$$i_{L1}(t) = \frac{-V_{m1}}{L_1}(t - t_0) + i_{L1}(t_0) \quad t_0 \leq t < t_1 \quad (2)$$

where  $i_{L1}(t_0)$  is the initial current in  $L_1$  at  $t = t_0$

Similarly, the voltage and current in inductor  $L_1'$  are expressed as

$$v_{L1}' = V_{DC} - V_{m1} = L_1' \frac{di_{L1}'}{dt} \quad t_0 \leq t < t_1 \quad (3)$$

$$i_{L1}'(t) = \frac{V_{DC} - V_{m1}}{L_1'}(t - t_0) + i_{L1}'(t_0) \quad t_0 \leq t < t_1 \quad (4)$$

where  $i_{L1}'(t_0)$  is the initial current in  $L_1'$  at  $t = t_0$ .

The main lamp-1 current is expressed as

$$i_{m1}(t) = i_{L1}(t) + i_{L1}'(t) \quad (5)$$

From Eqn. (2) and Eqn. (4), the ripple current in  $L_1$  and  $L_1'$  are expressed as

$$\Delta i_{L1} = i_{L1}(t_1) - i_{L1}(t_0) = \frac{-V_{m1}}{L_1}(t_1 - t_0) = \frac{-V_{m1}}{L_1} DT_s \quad (6)$$

$$\Delta i_{L1}' = i_{L1}'(t_1) - i_{L1}'(t_0) = \frac{V_{DC} - V_{m1}}{L_1'}(t_1 - t_0) = \frac{V_{DC} - V_{m1}}{L_1'} DT_s \quad (7)$$

Where  $DT_s$  is the ON period of switches  $S_1$  &  $S_4$ ,  $D$  is duty ratio and  $T_s$  is the switching period.

When switches  $Q_2$  and  $Q_3$  are ON, inductor  $L_1$  charges linearly from  $V_{DC}$  and inductor  $L_1'$  gives its stored energy to lamp-1 through  $Q_3$ . From the Figure 5(a), the voltage and current in  $L_1$  are expressed as

$$v_{L1} = V_{DC} - V_{m1} = L_1 \frac{di_{L1}}{dt} \quad t_2 \leq t < t_3 \quad (8)$$

$$i_{L1}(t) = \frac{V_{DC} - V_{m1}}{L_1}(t - t_2) + i_{L1}(t_2) \quad t_2 \leq t < t_3 \quad (9)$$

Where  $i_{L1}(t_2)$  is the initial current in  $L_1$  at  $t = t_2$

Similarly, the voltage and current in  $L_1'$  are represented as

$$v_{L1}' = -V_{m1} = L_1' \frac{di_{L1}'}{dt} \quad t_2 \leq t < t_3 \quad (10)$$

$$i_{L1}'(t) = \frac{-V_{m1}}{L_1'}(t - t_2) + i_{L1}'(t_2) \quad t_2 \leq t < t_3 \quad (11)$$

Where  $i_{L1}'(t_2)$  is the initial current in  $L_1'$  at  $t = t_2$

From  $t_2 - t_3$ , main lamp-1 current is expressed as

$$i_{m1}(t) = i_{L1}(t) + i_{L1}'(t) \quad (12)$$

From Eqn. (9) the ripple current in inductor  $L_1$  is expressed as

$$\Delta i_{L1} = i_{L1}(t_3) - i_{L1}(t_2) = \frac{V_{DC} - V_{m1}}{L_1}(t_3 - t_2) = \frac{V_{DC} - V_{m1}}{L_1}(1 - D)T_s \quad (13)$$

From (11), the ripple current in inductor  $L_1'$  is given as

$$\Delta i_{L1}' = i_{L1}'(t_3) - i_{L1}'(t_2) = \frac{-V_{m1}}{L_1'}(t_3 - t_2) = \frac{-V_{m1}}{L_1'}(1 - D)T_s \quad (14)$$

Where  $(1-D)T_s$  is the OFF period of switches  $Q_1$  &  $Q_4$  and  $T_s$  is the switching period. The voltage across lamp-1 can be obtained by applying volt-sec balance either on  $L_1$  or  $L_1'$

$$[i_{L1}'(t_1) - i_{L1}'(t_0)] + [i_{L1}'(t_3) - i_{L1}'(t_2)] = 0 \text{ (or)}$$

$$[i_{L1}(t_1) - i_{L1}(t_0)] + [i_{L1}(t_3) - i_{L1}(t_2)] = 0 \quad (15)$$

$$\frac{-V_{m1}}{L_1}DT + \frac{V_{DC} - V_{m1}}{L_1}(1 - D)T = 0 \text{ (or)} \frac{V_{DC} - V_{m1}}{L_1'}DT + \frac{-V_{m1}}{L_1'}(1 - D)T = 0 \quad (16)$$

$$V_{m1} = (1 - D)V_{DC} \text{ (or)} V_{m1} = DV_{DC} \quad (17)$$

The similar analysis is applicable for main lamp-2, thus  $\Delta i_{L2}$ ,  $\Delta i_{L2}'$  and  $V_{m2}$  are given as

$$\Delta i_{L2} = \frac{V_{DC} - V_{m2}}{L_2}DT = \frac{-V_{m2}}{L_2}(1 - D)T \quad (18)$$

$$\Delta i_{L2}' = \frac{-V_{m2}}{L_2'}DT = \frac{V_{DC} - V_{m2}}{L_2'}(1 - D)T \quad (19)$$

$$V_{m2} = (1 - D)V_{DC} \text{ (or)} DV_{in} \quad (20)$$

Under continuous current for selected current ripple, the values of ( $L_1$  &  $L_1'$ ) can be calculated from Eqn. (13) and (14) respectively, similarly, values of ( $L_2$  &  $L_2'$ ) can be calculated from Eqn. (18) and (19) respectively.

## B. Analysis of Local Lighting System

Local LED lighting system consists of two strings; local LED string-1 and local LED string-2. To derive the relation between  $V_{LLS} - V_{DC}$ , an equivalent circuit shown in Figure 5 (b) is considered. In the proposed configuration, FBI output voltage ( $V_{AC}$ ), which is a square wave, is given to series resonant circuit (SRC) that produces sinusoidal resonant current ( $i_r$ ). Therefore, the relation between  $V_{LLS} - V_{DC}$  is derived using conventional ac analysis. SRC allows only fundamental voltage component of  $V_{AC}$ . The  $R_{ac}$  is the ac resistance between the terminals B and C. The  $X_{Lr}$  and  $X_{Cr}$  denote the reactance offered by  $L_r$  and  $C_r$  respectively. From Figure 5(b), the relation between  $V_{LLS} - V_{DC}$  is calculated as

$$\frac{V_{AC}}{V_{BC}} = \frac{R_{ac}}{R_{ac} + j(X_{Lr} - X_{Cr})} = \frac{1}{\left[1 + j\left(\frac{X_{Lr} - X_{Cr}}{R_{ac}}\right)\right]} \quad (21)$$

$V_{AC}$  and  $V_{BC}$  are the fundamental voltage components present in the square wave voltage of magnitude  $V_{DC}$  and  $V_{LLS}$  respectively. From Figure 5(b), the ac resistance  $R_{ac}$  can be calculated [20] and is given by.

$$R_{ac} = \frac{8}{\pi^2} R_{LLS} \quad (22)$$

Where  $R_{LLS}$  is the dc resistance offered by local LED strings.

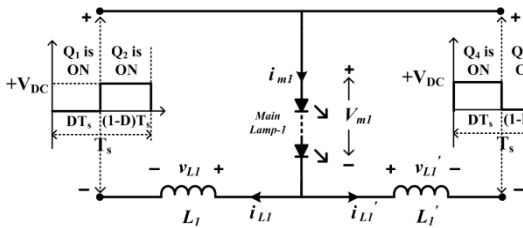


Figure 5 (b). Simplified circuit for the analysis of main lamp-1.

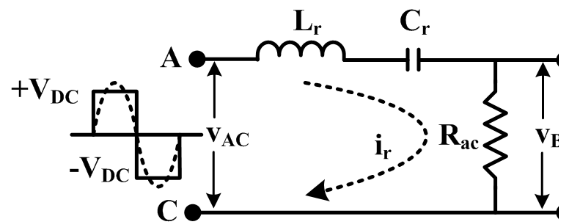


Figure 5 (b). AC equivalent circuit for the analysis of local LED strings.

The quality factor ( $Q$ ) of SRC is defined by

$$Q = \frac{\omega_0 L_r}{R_{LLS}} = \frac{1}{\omega_0 C_r R_{LLS}} \quad (23)$$

Where  $\omega_0$  is resonant frequency and it is given by

$$\omega_0 = 2\pi f_0 = \frac{1}{\sqrt{L_r C_r}} \text{ rad/sec} \quad (24)$$

From Eqn. (24),  $f_0$  is represented as

$$f_0 = \frac{1}{\left[2\pi\sqrt{L_r C_r}\right]} \text{ Hz} \quad (25)$$

And,

$$X_{L_r} = 2\pi f_s L_r \quad (26)$$

$$X_{C_r} = \frac{1}{2\pi f_s C_r} \quad (27)$$

After substituting Eqn. (23), (23), (26) and (27) in Eqn. (21), the relation between  $V_{LLS} - V_{DC}$  is finally calculated as

$$\frac{V_{AC}}{V_{BC}} = \frac{4V_{LLS}/\pi}{4V_{DC}/\pi} = \frac{V_{LLS}}{V_{DC}} = \frac{1}{\left[1 + j\frac{\pi^2}{8}Q\left(\frac{f_s}{f_0} - \frac{f_0}{f_s}\right)\right]} \quad (28)$$

#### 4. Design considerations

##### A. Main lighting system and its parameters:

Two identical main lamps are used in the proposed configuration and they are powered through interleaving concept. The rating of main lamps, calculation of interleaved inductor values and input voltage are presented in section. Equivalent circuit [21] of an LED is required to select the parameters related main lighting system. In this research work, TMX HP 3WLEDs are used. The v-i characteristics of TMX HP 3WLED are shown in Figure 6. From the characteristics, it is found that cut-in voltage ( $V_{th}$ ) of LED is 2.3 V, and an operating point at forward voltage ( $V_F$ ) equal to 3.42 V and forward current ( $I_F$ ) equal to 0.59 A is chosen. Each main lamp is comprised of four strings and seven series LEDs in each string. Therefore each main lamp is operated at 23.94 V, 2.36 A and 56 W. And,  $V_{th}$  of each main lamp is obtained as 16.1 V. It is observed that output voltage ( $V_{m1}$  or  $V_{m2}$ ) of each main lamp is obtained as 23.94 V and output current ( $i_{m1}$  or  $i_{m2}$ ) through each main lamp is 2.36 A.

Referring equation (17) and (20), input voltage  $V_{DC}$  is given by

$$V_{DC} = \frac{V_{m1}}{D} \text{ (or)} \frac{V_{m2}}{1-D} \quad (29)$$

With a duty ratio (D) of 0.5, and a  $V_{m1}$  (or)  $V_{m2}$  of 23.94 V, the input voltage is calculated by

$$V_{DC} = \frac{23.94}{0.5} \cong 48 \text{ V}$$

As the main lamps are identical, each interleaved inductor ( $L_1$  or  $L_1'$  or  $L_2$  or  $L_2'$ ) supplies half

*Nanotechnology Perceptions* Vol. 20 No. S10 (2024)

of the main lamp current. Interleaved inductor value depends on switching frequency, duty ratio and allowable ripple current. In the proposed configuration, ripple current allowed in each interleaved inductor is same. Hence equation (19) is used to calculate inductor value and  $L_2$  is given by

$$L_2' = \frac{V_{DC} - V_{m1}}{\Delta i_{L2}'} (1 - D)T \quad (30)$$

With a  $V_{DC}$  of 48 V, a  $V_{m1}$  of 23.94 V, a  $D$  of 0.5, a switching period  $T_s$  of 8  $\mu$ s, and the current ripple  $\Delta i_{L2}'$  is taken as 1.203 A, the inductor  $L_2$  is given by

$$L_2' = \frac{(48 - 23.94)}{(1.203)} \cdot (1 - 0.5) \cdot 8 \cdot 10^{-6} \cong 80 \mu\text{H} = L_2 = L_1 = L_1'$$

#### B. Local lighting system and its parameters:

Two identical LED strings are connected in parallel in local lighting system and are supplied through series resonant circuit. In this section, section of local LED string rating, calculation of SRC parameters and input voltage are provided. For an LED in each string, an operating point at  $V_F = 3.42$  V and  $I_F = 0.59$  A is selected. Each string is comprised of 14 series LEDs. Therefore, each local LED string is operated at  $V_{LLS} = 47.88$  V,  $i_{LLS1}$  or  $i_{LLS2} = 0.59$  A and 28 W. And,  $V_{th}$  of each local LED string is obtained as 32.2 V. In this converter, resonant frequency ( $f_0$ ) doesn't need to be less than switching frequency ( $f_s$ ) to achieve zero-voltage switching (ZVS) transition during dead time. A constant current during dead time is provided by interleaved inductors. Hence converter operating frequency (125 kHz) is equal to resonant frequency. Referring equation (25), resonant inductor ( $L_r$ ) and capacitor ( $C_r$ ) are selected as 50  $\mu$ H and 33 nF respectively. From equation (28), at  $f_s = f_0$ , the input voltage ( $V_{DC}$ ) becomes equal to voltage across local LED string ( $V_{LLS}$ ). Therefore  $V_{DC} \approx 48$  V. The switch output capacitors of proposed converter play a crucial role to obtain zero voltage switching. These values are calculated by using capacitor basic v-i relation with assumptions (i) current flowing through the interleaved inductors are constant and (ii) dead time  $t_{d1}$  is same as dead time  $t_{d2}$  and both are represented as  $t_d$ .

The current through switch output capacitors during  $t_{d1}$  or  $t_{d2}$  is obtained as follows,

$$\Delta i_{L1,2,1',2'} = \frac{2C_m V_{DC}}{t_d}, \text{ where } m = 1, 2, 3, 4 \quad (31)$$

For a  $t_d$  value of 100 ns,  $C_m$  can be found as from (31)

$$C_m = \frac{(1.203)(100)(10^{-9})}{(2)(48)} \cong 1250 \text{ pF}$$

For proper ZVS,  $C_m$  is selected a small value than the obtained because dead time is fixed between gate signals.

### 5. Regulation and Dimming Control of Proposed Converter

The proposed converter is designed to operate with fixed duty cycle control, therefore the main and local loads must be regulated against the variations in  $V_{in1}$ , and  $V_{in2}$ . The input voltage  $V_{DC}$  to the proposed converter is obtained from three dc voltages  $V_{in1}$ ,  $V_{in2}$ , and  $V_C$  instead of being supplied directly. The variations in  $V_{in1}$ , and  $V_{in2}$  are compensated by buck-boost converter by controlling duty cycle of  $Q_B$ .

In this converter, main lamps are operated at full illumination. However each local LED string is dimmed independently using pulse width modulation (PWM) technique. A switch  $S_{dim1}$  is connected in series with LLS-1 and  $S_{dim2}$  is connected in series with LLS-2. Both  $S_{dim1}$  and  $S_{dim2}$  are operated at low frequency (100 Hz) and their turn-on duration decides the average current through local LED strings.

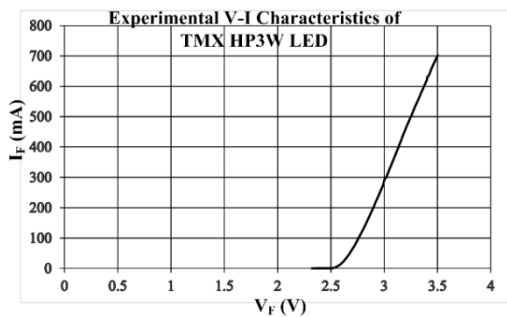


Figure 6. TMX HP-3W LED characteristics.

Table. I Specifications of proposed configuration

Parameter	Value
Input Voltage $V_{DC}$	48 V
Inductors, $L_{1,2,1',2'}$	80 $\mu$ H
Resonant Inductor, $L_r$	50 $\mu$ H
Resonant Capacitor, $C_r$	33 nF
Switching frequency, $f_s$	125 kHz
Main lamp Voltages, $V_{m1, m2}$	23.94 V
Main lamp Currents, $i_{m1, m2}$	2.36 A
Local String Voltage, $V_{LLS}$	47.88 V
Local String Current, $i_{LLS1,2}$	0.59 A

### 6. Results and Discussion

The simulation of the proposed converter for local and main LED lighting application shown in Figure 1 is performed using OrCAD PSpicesimulation environment. The specifications of proposed configuration are shown in Table. I.

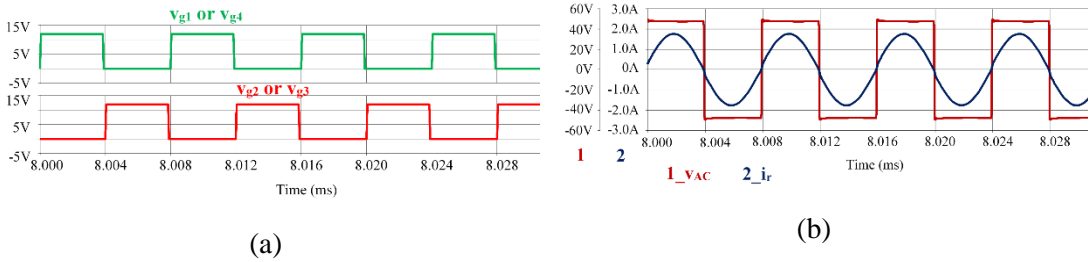


Figure 7. Simulation waveforms. (a) Gate voltages of switches in FBI. (b) Output voltage and resonant current in FBI.

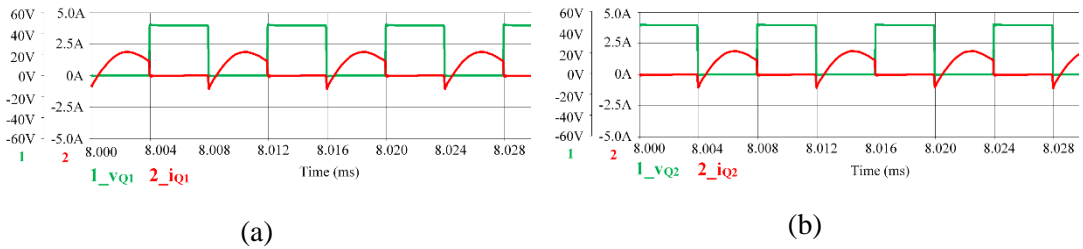
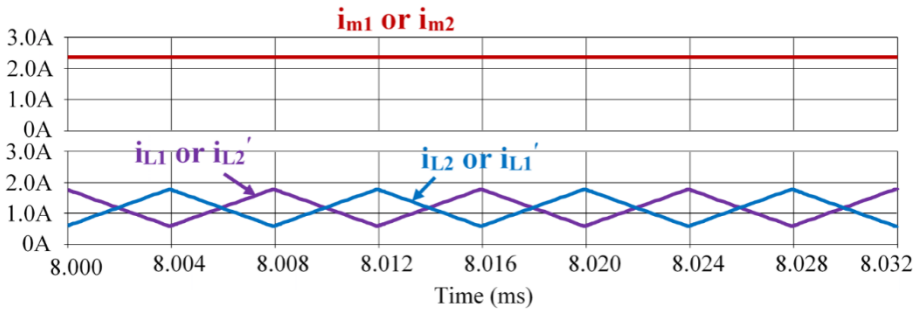
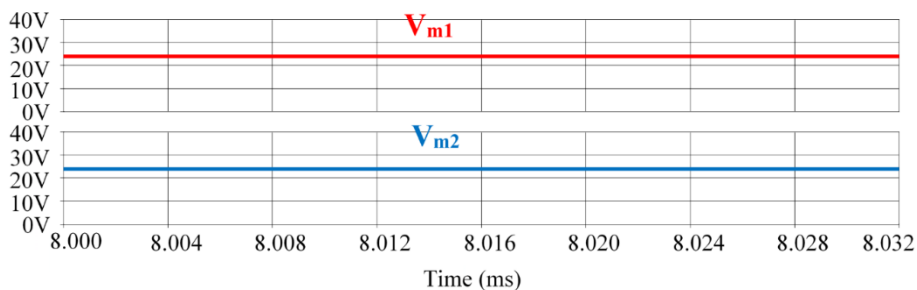


Figure 8. Switching waveforms. (a)  $v_{Q1}$  and  $i_{Q1}$ . (b)  $v_{Q2}$  and  $i_{Q2}$ .

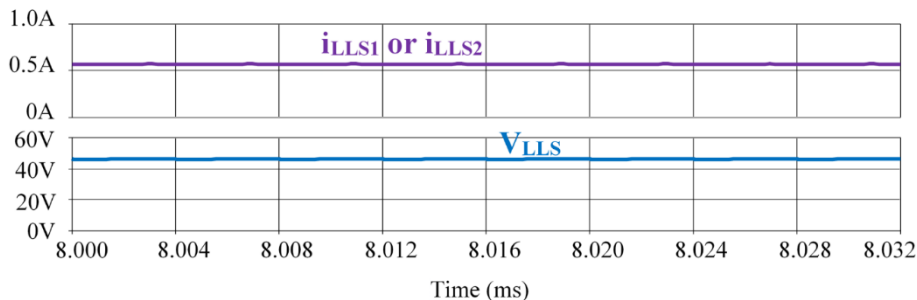
The input voltage applied to FBI is 48 V. Each main LED lamp is designed to operate at 56 W and each local LED string is designed to operate at 28 W. Figure 7(a) shows the waveforms of gate voltages of switches of FBI. Figure 7(b) shows the corresponding output voltage and resonant current in FBI. It is observed that both main and local lightings are powered with equal duty ratio i.e.,  $D = 0.5$  and  $(1 - D) = 0.5$ . At this condition, the switching waveforms of FBI devices are shown in Figure 8. It is clearly noted that turn ON and turn OFF switching transitions are accomplished at zero voltage. Figure 9 shows current through each interleaved inductor, output voltage and current of main lamps, and local LED strings at full illumination. It is shown that the main lamp voltages ( $V_{m1}$  &  $V_{m2}$ ) and currents ( $i_{m1}$  &  $i_{m2}$ ) are at selected value without ripple. Similarly, local LED string voltage ( $V_{LLS}$ ) and currents ( $i_{LLS1}$  &  $i_{LLS2}$ ) are also at selected value. At this power, the efficiency of the proposed converter configuration is found to be 94.74%.



(a) Currents in interleaved inductors



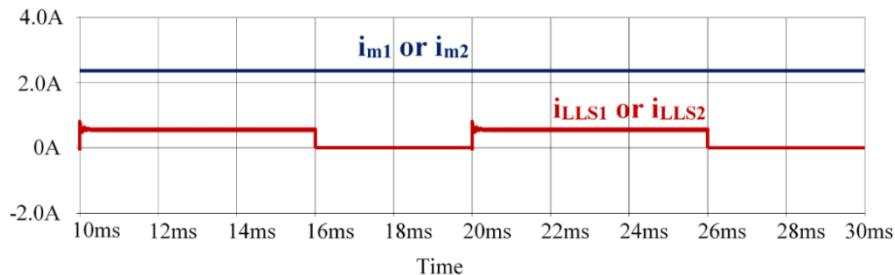
(b) Output voltage of main lamps



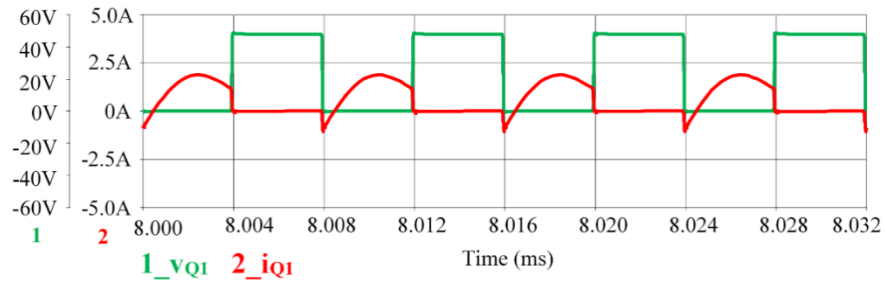
(c) Output voltage and current of local LED strings

Figure 9. Voltage and current waveforms of main and local lighting systems

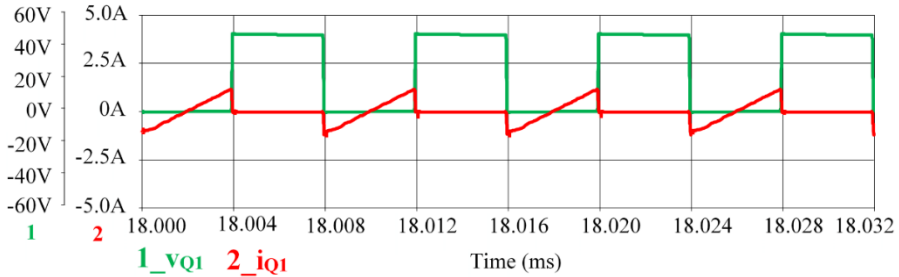
In this converter, main lamps are operated at selected power level continuously. To show the dimming feature in local LED strings, both LLS-1 and LLS-2 are operated at 60% of selected power level by using corresponding dimming switches ( $S_{dim1}$  &  $S_{dim2}$ ). Figure 10(a) shows current through main lamp and local LED strings. It is observed that the main lamp currents ( $i_{m1}$  &  $i_{m2}$ ) are at selected value, but local LED string currents ( $i_{LLS1}$  &  $i_{LLS2}$ ) are also at 60% of selected value. Figure 10(b) and (d) show the voltage and current in switch  $Q_1$  &  $Q_2$  when  $S_{dim1}$  &  $S_{dim2}$  are ON. Figure 10(c) and (e) show the voltage and current in switch  $Q_1$  &  $Q_2$  when  $S_{dim1}$  &  $S_{dim2}$  are OFF. It is clearly evident that switches in FBI are switched at zero voltage. At this power, the efficiency of the proposed converter configuration is found to be 95.63%. A slight increase in efficiency is due to the reduction in conduction losses of devices in FBI.



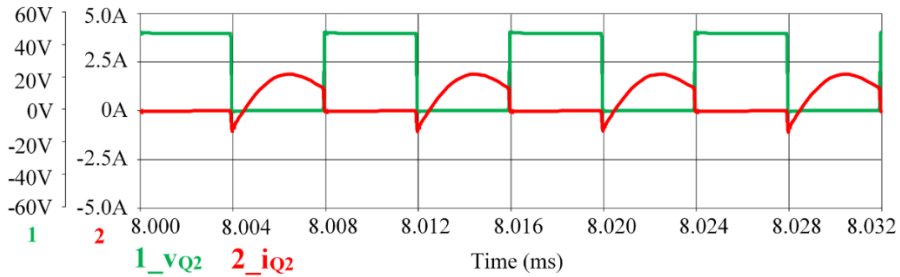
(a) Current through main lamp and local LED strings



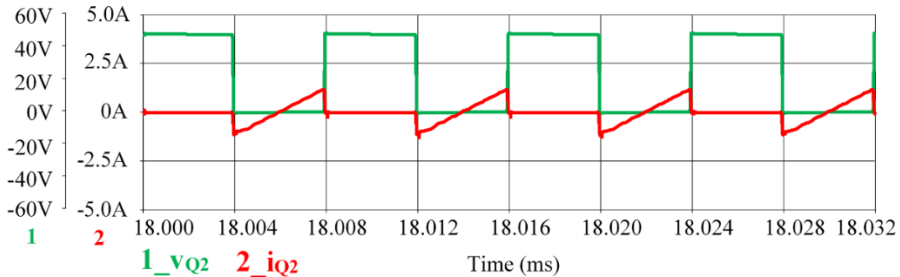
(b) Voltage and current in switch  $Q_1$  when  $S_{dim1}$  &  $S_{dim2}$  are ON



(c) Voltage and current in switch  $Q_1$  when  $S_{dim1}$  &  $S_{dim2}$  are OFF

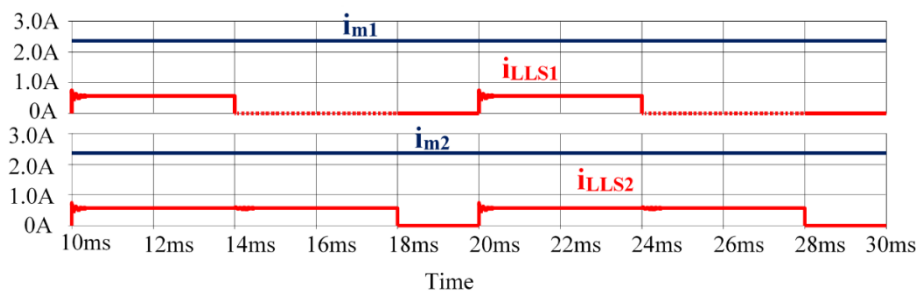


(d) Voltage and current in switch  $Q_2$  when  $S_{dim1}$  &  $S_{dim2}$  are ON

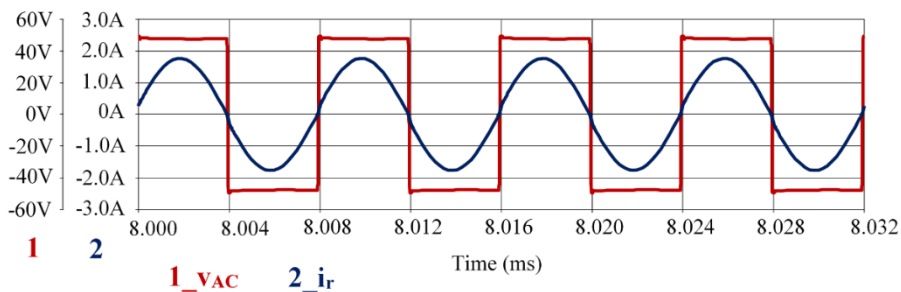


(e) Voltage and current in switch  $Q_2$  when  $S_{dim1}$  &  $S_{dim2}$  are OFF

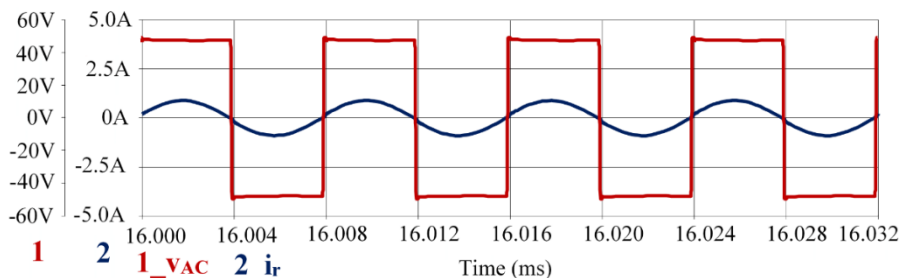
Figure 10. Currents in main and local lighting and switching waveforms at 60% dimming of both LLS1 & LLS2



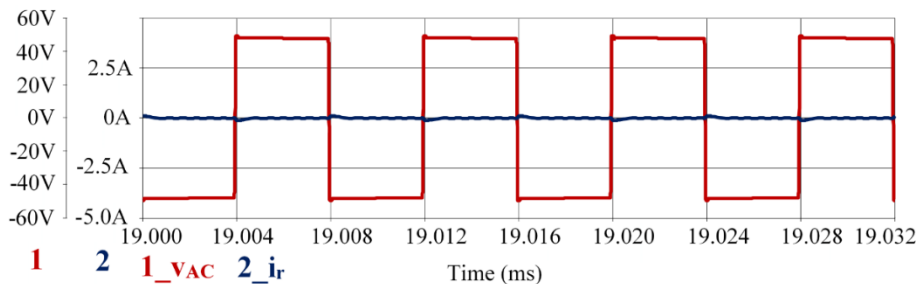
(a) Current through main lamp and local LED strings



(b)  $v_{AC}$  and  $i_r$  when  $S_{dim1}$  &  $S_{dim2}$  are ON



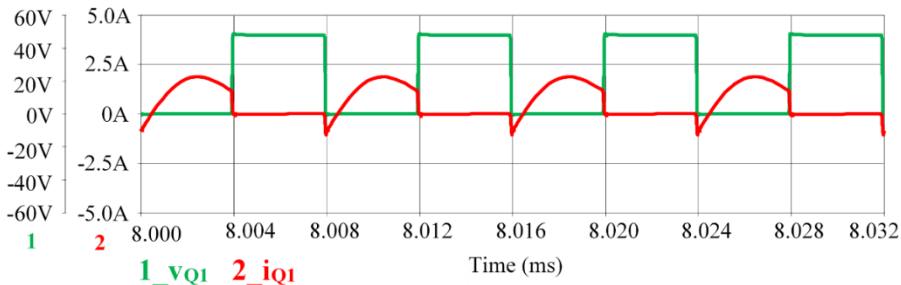
(c)  $v_{AC}$  and  $i_r$  when  $S_{dim1}$  is ON &  $S_{dim2}$  is OFF



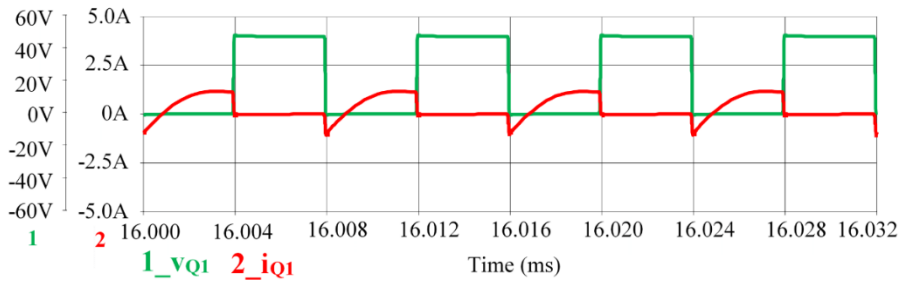
(d)  $v_{AC}$  and  $i_r$  when  $S_{dim1}$  is OFF &  $S_{dim2}$  is OFF

Figure 11. Currents in main and local lighting and switching waveforms at 40% dimming of LLS1 & 80% dimming of LLS2

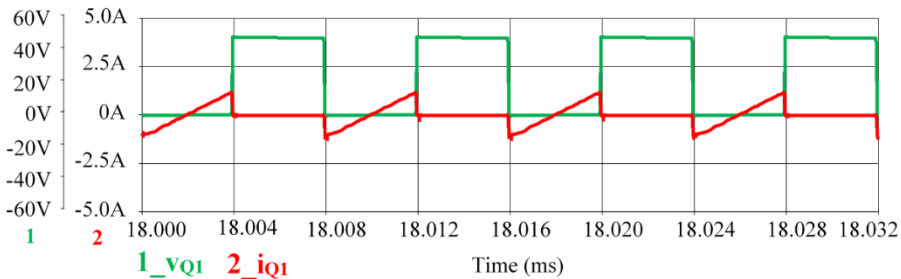
Independent dimming feature in local LED strings is also addressed. LLS-1 is operated at 40% of selected power level and LLS-2 are operated at 80% of selected power level by using  $S_{dim1}$  &  $S_{dim2}$ . Figure 11(a) shows current through main lamp and local LED strings. It is observed that the main lamp currents ( $i_{m1}$  &  $i_{m2}$ ) are at selected value but  $i_{LLS1}$  is at 40% and  $i_{LLS2}$  is at 60% of selected value. FBI output voltage ( $v_{AC}$ ) and resonant current ( $i_r$ ) when  $S_{dim1}=ON$  &  $S_{dim2}=ON$ ,  $S_{dim1}=ON$  &  $S_{dim2}=OFF$ , and  $S_{dim1}=OFF$  &  $S_{dim2}=OFF$  are shown in Figure 11(b), (c) and (d) respectively. It is observed that magnitude of  $i_r$  is decreased but  $f_s = f_0$  condition is maintained. To show soft-switching feature during independent dimming of local LED strings, voltage and current in switch  $Q_1$  when  $S_{dim1}=ON$  &  $S_{dim2}=ON$ ,  $S_{dim1}=ON$  &  $S_{dim2}=OFF$ , and  $S_{dim1}=OFF$  &  $S_{dim2}=OFF$  are shown in Figure 12(a), (b) and (c) respectively. It is clearly understood that  $Q_1$  is switched at zero-voltage. Further turn-on and off current magnitude during switching are not affected. At this power, the efficiency of the proposed converter configuration is found to be 95.87%.



(a) Voltage and current in switch  $Q_1$  when  $S_{dim1}$  &  $S_{dim2}$  are ON



(b) Voltage and current in switch  $Q_1$  when  $S_{dim1}$  is ON &  $S_{dim2}$  is OFF



(c) Voltage and current in switch  $Q_1$  when  $S_{dim1}$  &  $S_{dim2}$  are OFF

Figure 12. Switching waveforms at 40% dimming of LLS1 & 80% dimming of LLS2

## 7. Conclusions

In this research work, an integrated full-bridge series resonant converter is presented to power both local and main lighting systems. The ripple in voltage and current of main lighting system is very small due to inter-leaving concept. Local LED lighting system is powered through series LC resonance with independent dimming. For regulating main and local lighting against input voltage fluctuations, a buck-boost converter at the input side is used. The ZVS feature of devices in full-bridge converter is independent of local LED string currents. In addition conduction losses mainly depend on the magnitude of local LED string current. Therefore conduction and switching transition power losses are minimized which increase the proposed converter efficiency. This converter configuration may be suitable for applications like factory lighting, loco sheds, main office buildings, etc.

## References

1. Ramanjaneya Reddy U and Narasimharaju B. L, "Unity power factor buck-boost LED driver for wide range of input voltage application," 2015 Annual IEEE India Conference (INDICON), New Delhi, India, 2015, pp. 1-6, doi: 10.1109/INDICON.2015.7443347.
2. Ch, Kasi, Porpandiselvi Shunmugam and Vishwanathan Neti. An efficient full-bridge resonant converter for light-emitting diode (LED) application with simple current control. *International Journal of Circuit Theory and Applications*. 47. 10.1002/cta.2694.
3. M. Arias, I. Castro, D. G. Lamar, A. Vázquez and J. Sebastián, "Optimized Design of a High Input-Voltage-Ripple-Rejection Converter for LED Lighting," in *IEEE Transactions on Power Electronics*, vol. 33, no. 6, pp.5192-5205, June 2018, doi: 10.1109/TPEL.2017.2727343.
4. Kim, Jong-Woo, Jung-Muk Choe, and Jih-Sheng Jason Lai. "Non-isolated single-switch two-channel LED driver with simple lossless snubber and low-voltage stress." *IEEE Transactions on Power Electronics* 33.5 (2017): 4306-4316.
5. V. K. S. Veeramallu, S. Porpandiselvi and B. L. Narasimharaju, "A Nonisolated Wide Input Series Resonant Converter for Automotive LED Lighting System," in *IEEE Transactions on Power Electronics*, vol. 36, no. 5, pp. 5686-5699, May 2021, doi: 10.1109/TPEL.2020.3032159
6. M. Khatua et al., "High-Performance Megahertz-Frequency Resonant DC–DC Converter for Automotive LED Driver Applications," in *IEEE Transactions on Power Electronics*, vol. 35, no. 10, pp. 10396-10412, Oct. 2020.
7. A. Agrawal, K. C. Jana and A. Shrivastava, "A review of different DC/DC converters for power quality improvement in LED lighting load," 2015 International Conference on Energy Economics and Environment (ICEEE), 2015, pp. 1-6.
8. V. C. Bender, T. B. Marchesan and J. M. Alonso, "Solid-State Lighting: A Concise Review of the State of the Art on LED and OLED Modeling," in *IEEE Industrial Electronics Magazine*, vol. 9, no. 2, pp. 6-16, June 2015.
9. Y. Wang, J. M. Alonso and X. Ruan, "A Review of LED Drivers and Related Technologies," in *IEEE Transactions on Industrial Electronics*, vol. 64, no. 7, pp. 5754-5765, July 2017.
10. S. Li, S. -C. Tan, C. K. Lee, E. Waffenschmidt, S. Y. Hui and C. K. Tse, "A survey, classification, and critical review of light-emitting diode drivers," *IEEE Transactions on Power Electronics*, vol. 31, no. 2, pp. 1503-1516, Feb. 2016.
11. H. R. Kolla, N. Vishwanathan, and B. K. Murthy, "Input voltage controlled full-bridge series resonant converter for led driver application," *IET Power Electronics*, vol. 13, DOI 10.1049/iet-pel.2020.0554, no.19, p.4532-4541, Dec. 2020.
12. C. Kasi Ramakrishnareddy, S. Porpandiselvi, and N. Vishwanathan, "Soft switched full-bridge

- light emitting diode driver configuration for street lighting application,” IET Power Electronics, vol. 11, DOI 10.1049/ietpel.2017.0021, no. 1, pp. 149–159, 2018.
13. Kasi Ramakrishnareddy Ch, S. Porpandiselvi & N. Vishwanathan (2019) An efficient ripple-free LED driver with zero-voltage switching for street lighting applications, EPE Journal, 29:3, 120-131, DOI: 10.1080/09398368.2019.1570745
  14. V. K. S. Veeramallu, P. S., and N. B. L., “A buck-boost integrated high gain non-isolated half-bridge series resonant converter for solar pv/battery fed multiple load led lighting applications,” International Journal of Circuit Theory and Applications, vol. 48, pp. 266–285, 2020.
  15. U. Ramanjaneya Reddy and B. L. Narasimharaju, “A cost-effective zero-voltage switching dual-output led driver,” IEEE Transactions on Power Electronics, vol. 32, DOI 10.1109/TPEL.2016.2636244, no. 10, pp. 7941–7953, Oct. 2017.
  16. Mounika D, Vishwanathan N & Porpandiselvi S (2020): A level shifted asymmetric duty cycle controlled half-bridge series resonant LED driver configuration, EPE Journal, DOI: 10.1080/09398368.2020.1725858
  17. J. M. Alonso, M. S. Perdigão, M. A. Dalla Costa, G. Martínez and R. Osorio, "Analysis and Experiments on a Single-Inductor Half-Bridge LED Driver With Magnetic Control," in IEEE Transactions on Power Electronics, vol. 32, no. 12, pp. 9179-9190, Dec. 2017.
  18. K. R. Ch, S. Porpandiselvi, and N. Vishwanathan, “A three-leg resonant converter for two output led lighting application with independent control,” International Journal of Circuit Theory and Applications, vol. 47, DOI 10.1002/cta.2632, no. 7, pp.1173-1187.
  19. H. R. Kolla, N. Vishwanathan and B. K. Murthy, "Independently Controllable Dual-Output Half-Bridge Series Resonant Converter for LED Driver Application," in IEEE Journal of Emerging and Selected Topics in Power Electronics, vol. 10, no. 2, pp. 2178-2189, April 2022.